Evidence of neotectonic reactivation of the Katrol Hill Fault during late Quaternary and its GPR characterization

A. K. Patidar[1], D. M. Maurya[1,*], M. G. Thakkar[2] and L. S. Chamyal[1]

[1]Department of Geology, M.S. University of Baroda, Vadodara 390 002, India
[2]Department of Geology, R.R. Lalan College, Bhuj, Kachchh 370 001, India

The Katrol Hill Fault (KHF) is an E–W trending major intrabasinal fault located in the central part of Mainland Kachchh. Several lines of geomorphic evidence suggest periodic reactivation of the KHF during the Quaternary period. The present study is based on geomorphic investigations along the entire length of the KHF and detailed analysis of Quaternary faulting observed supplemented with ground penetrating radar (GPR) investigations. The dip of the KHF is observed between 45° and 80° due south within the Mesozoic formations, reducing to 40–45° in the overlying Quaternary deposits. Offsetting in Quaternary sediments overlying the KHF indicate three events of faulting during the late Quaternary. Based on the stratigraphic set-up of Quaternary sediments, it is suggested that Event 1 occurred sometime in the late Pleistocene, while the Events 2 and 3 took place during early Holocene and <2 ka respectively. The reverse movement indicated by faulting in Quaternary sediments, splaying nature of the fault as revealed by GPR and changes in the geometry of the fault towards the surface indicate periodic reactivation of the KHF in compressive stress regime.

Keywords: Ground penetrating radar, Kachchh, Katrol Hill Fault, Quaternary reactivation, tectonic geomorphology.

THE Kachchh rift basin, located at the western extremity of India, opened during the Early Jurassic, and became fully marine in Middle Jurassic which resulted in the deposition of more than 2000–3000 m thick Mesozoic and Cenozoic sediment succession[1,2]. The framework of the present fault-controlled geomorphic configuration of Kachchh is attributed to inversion of the basin in the late Cretaceous[2,3]. In general, the post-rift (inversion phase) geological evolution of the basin is marked by periodic reactivation of various E–W-trending intrabasinal faults like the Island Belt Fault (IBF), Kachhh Mainland Fault (KMF), South Wagad Fault (SWF), Katrol Hill Fault (KHF) and others (Figure 1), which are also responsible for recurrent seismic activity in the region[4]. It is therefore essential to characterize the active faults of the area and their precise subsurface investigations to document the successive tectonic events and related landform development during the Quaternary.

The present study deals with the E–W trending KHF that marks the northern boundary of the Katrol hill range in the central part of the Mainland Kachchh. The Katrol hill range corresponds to the flexure zone to the south of the KHF with the rocky plain of Bhuj to the north. The Mesozoic sequence of Mainland Kachchh is divided into four formations named as the Jhurio (Jhura), Jumara, Jhuran and Bhuj formations in ascending order[1,2]. In the Katrol hill range, the Jumara and Jhuran formations show higher degree of deformation, as evidenced by the E–W trending asymmetrical domal and anticlinal structures, which are truncated over the KHF[1,2], illustrating the compressive stress regime (Figures 1 and 2). The southern limbs of the flexures show inclination of ~5–10°, while the northern limbs are steeply dipping to vertical and terminate against the KHF[1,2]. Several N–S, NNE–SSW, NNW–SSE-trending igneous intrusive dykes cut across these domes and deform the country rocks[1]. The KHF also exhibits lateral offsetting along NNE–SSW and NNW–SSE-trending transverse faults[5,6]. Here, we discuss the tectonic geomorphology and Quaternary sediments along the KHF, delineate its structural characteristics and provide evidence of its reactivation during late Quaternary (Figure 1). The results of geomorphic, stratigraphic and Ground Penetrating Radar (GPR) studies are synthesized to interpret the tectonic behaviour of the KHF in the recent past.

Geomorphology of the Katrol Hill Fault

The E–W-trending KHF is a major range-bounding fault that divides the Mainland Kachchh into the northern and southern parts. Geomorphologically, the KHF is expressed as an E–W-trending line of north-facing scarps separating the rocky plain comprising sandstones of Bhuj Formation to the north and the rugged terrain of Katrol hill range made up of highly deformed Mesozoic rocks older than the Bhuj Formation. The KHF, therefore, marks a sharp lithotectonic contact between the Bhuj Formation

*For correspondence. (e-mail: dmmaurya@yahoo.com)

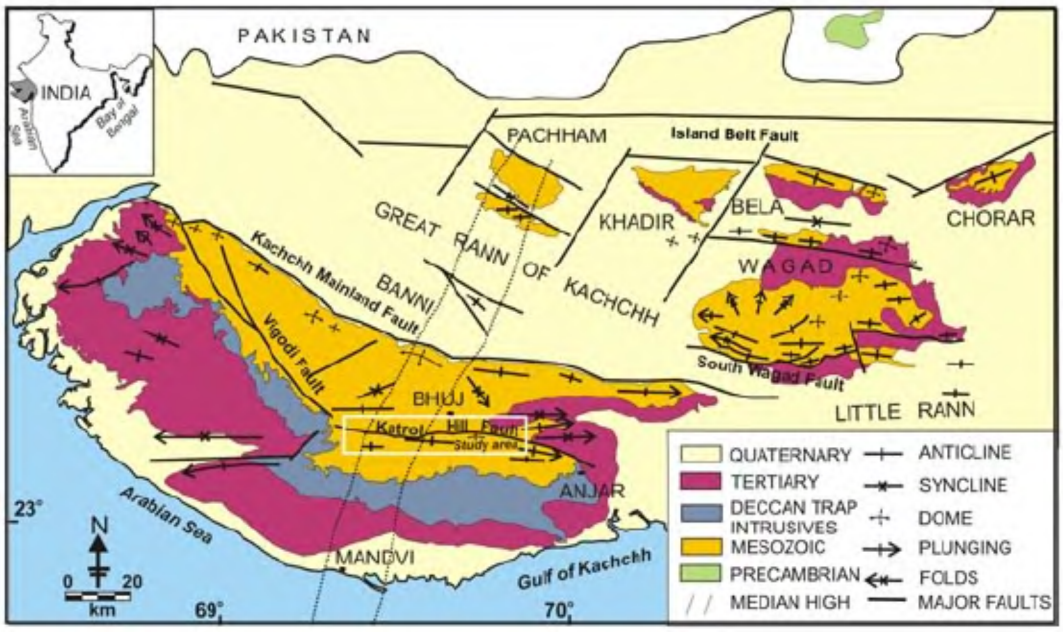

Figure 1. Generalized tectonic map of Kachchh showing various faults and associated structures (after Biswas and Deshpande[24]).

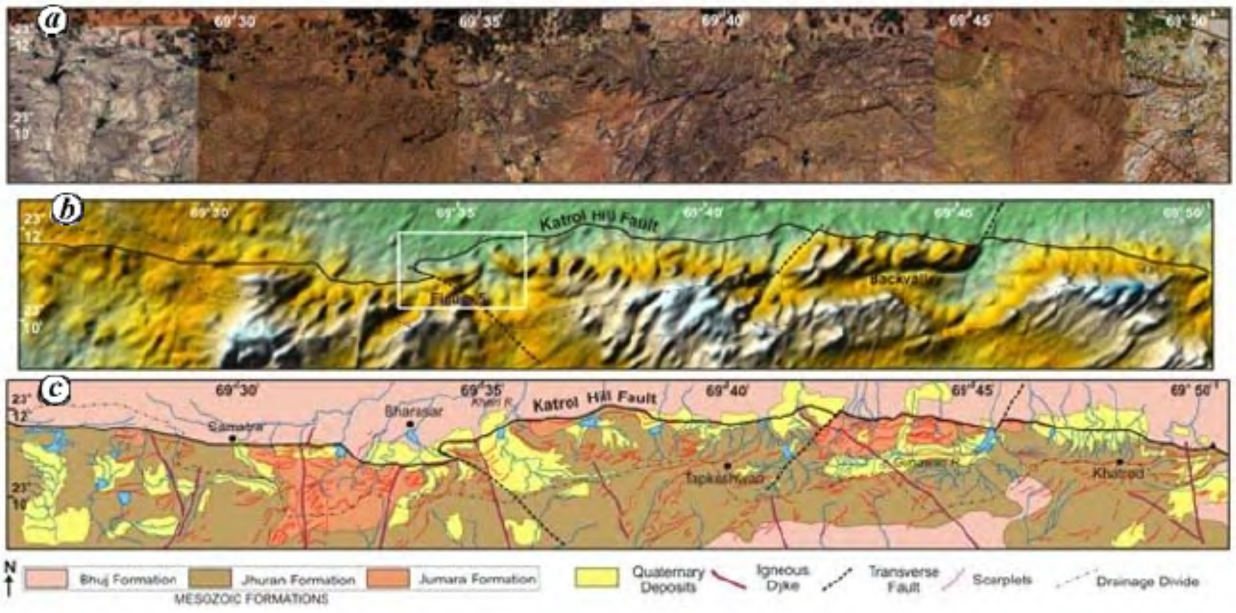

Figure 2. ***a***, Satellite image of the Katrol hill range illustrating geomorphology and structural set-up (source: www.googleearth.com). ***b***, Digital terrain model of the Katrol hill range showing sharp geomorphic contrast across the KHF. The trace of KHF is based on Patidar *et al.*[6]. ***c***, Geological map of the Katrol hill range prepared using satellite image and field mapping. Note the KHF marking the lithotectonic contact between the Bhuj Formation in the north and the older Mesozoic rocks in the south and the distribution of Quaternary deposits.

and older Mesozoic formations like the Jhuran and Jumara that form a narrow zone of domal structures along the KHF. Field investigations and mapping of the KHF using GPR carried out by us earlier[6] suggest significant variation in the dip and strike of the fault plane. In the eastern part, the dip of the fault is 80° near Khatrod, which decreases towards the west up to 45° at Samatra (Figure 3). Though the general trend of the KHF is E–W, it shows significant variation in strike in the vicinity of transverse faults (Figure 2). The fault displays slight variation in

Figure 3. Field photographs of the fault plane of the KHF showing variation in the amount of dip of the fault from east to west. ***a***, SE of Samatra; ***b***, South of Bharasar; ***c***, North of Tapkeshwari; ***d***, North of Khatrod peak.

strike around Samatra also, which is possibly related to the changes in the attitude of the fault plane. Recent GPR-based studies have shown that the KHF is a steep, south-dipping reverse fault near the surface, which becomes vertical at depth[6,7]. The Jumara and Jhuran formations exposed within the rugged topography of the Katrol hill range form the hanging wall, which overrides the younger Bhuj Formation forming the footwall to the north[6,7].

The Digital Elevation Model (DEM) of Katrol hill range depicts abrupt changes in the elevation of the hanging wall of the KHF (Figure 4). The crest line comprising the highest summits of this range lies close to the northern edge, whereas the drainage divide to the south also lies close to the crestline. The DEM illustrates the narrow incised region between the crestline and drainage divide marked as backvalley trending E–W within the south-dipping Mesozoic formations (Figure 2 *a*). This backvalley is filled with Quaternary deposits, mostly by valley-fill miliolites. The offsetting of the range front scarp of the KHF along various transverse faults is clearly seen in the DEM. The Katrol hill range forms the main watershed of the Mainland Kachchh, the major rivers draining towards north are the Khari, Pat and Pur. Various domes situated to the south of KHF locally give rise to radial drainage pattern. The various rivers show narrow gorges of varying depth in Quaternary as well as in Mesozoic rocks. The short and straight river courses in the direction of the tectonic slope and the incised and confined channel belts indicate vertical uplift of the area.

Stratigraphy of Quaternary deposits along KHF

Quaternary deposits occur both within the Katrol hill range and to the north of the scarp overlapping the KHF. Though the deposits show patchy occurrences, a well-defined sequence of depositional phases can be recognized. The sequence of the Quaternary deposits starts with the bouldery colluvium, aeolian miliolite, valley-fill miliolite, alluvium and scarp-derived colluvium (Table 1). These Quaternary deposits are incised by various north-flowing rivers. The bouldery colluvium contains large fragments of shale and sandstone and is overlain by miliolites along the Katrol hill range. The miliolite deposits of the area are separated into two categories. The older miliolites occur on hill slopes which comprise well-lithified, fine-grained miliolitic sand and is of aeolian origin. They also occur as obstacle dunes and occupy topographic depressions and hollows in the slopes of high hills and ridges. The valley-fill miliolite occurs along incised cliffs and shows stratification with pebble-to-cobble size clasts of Mesozoic rocks, suggesting the role of fluvial activity in their deposition[6]. Valley-fill miliolites are also found in the backvalleys created within the Katrol hill range between the crestline and drainage divides. Since they are derived from carbonate-rich sand from miliolite rocks, these deposits show varying degrees of compaction[6]. The fine-grained alluvial deposits are found to overlie the miliolites and occur in patches within the Katrol hill range along various river valleys. The scarp-derived colluvium is the youngest Quaternary deposit of the area and

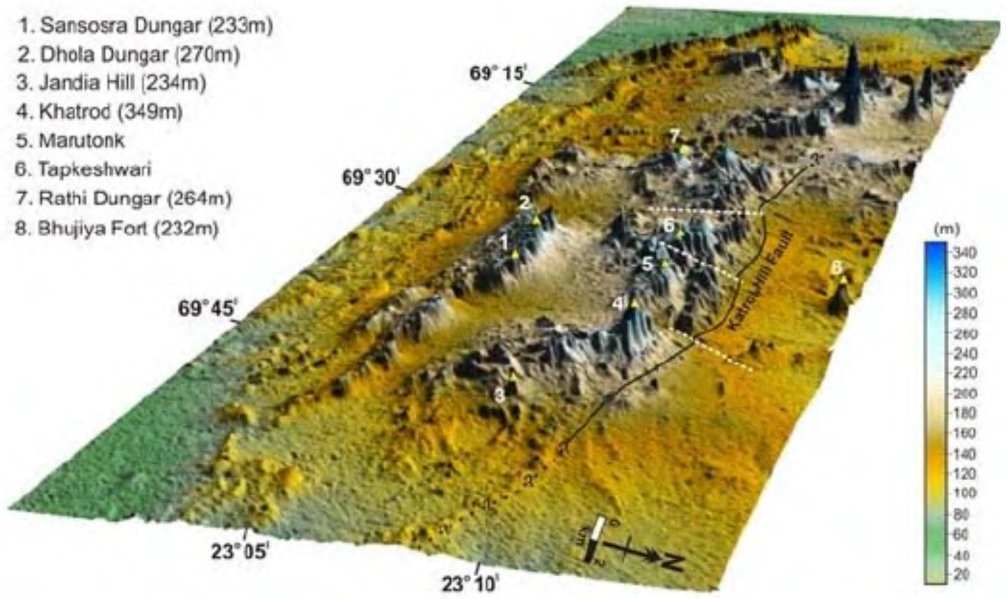

Figure 4. Digital elevation model showing southerly tilted rugged topography of the Katrol hill range. Note the sharp geomorphic contrast between the rocky plain of Bhuj and older Mesozoic formations. The KHF and transverse faults are marked on the basis of field and GPR investigations.

Table 1. Stratigraphy of Quaternary deposits along the Katrol hill range (based on Patidar *et al.*[6])

Quaternary deposits	Lithology	Occurrence	Age
Scarp-derived colluvium	Angular to sub-angular pebbles and cobbles embedded in sandy to gravelly matrix	At the base of range front scarp	Late Holocene
Alluvial deposits	Fine sand, silt and clay	Sporadically along the various north-flowing streams	Middle Holocene
Valley-fill miliolite	Sandy sheets of miliolite with boulders and pebbles	Extensively deposited along river valleys	Late Pleistocene
Aeolian miliolites	Well-sorted, fine-grained, carbonate-rich sand	At higher elevations along the southerly directed slopes of the hill range and at the base of the north-facing range front scarp	
Bouldery colluvial deposits	Boulder-size fragments of shale and sandstone	At the base of range front scarp	Middle Pleistocene

is found at the base of the range front scarp. The deposit shows a maximum thickness of 2–3 m along various north-flowing rivers. $^{230}Th/^{234}U$ ages of the miliolites occurring in the Katrol hill range vary from 130 to 30 ka, suggesting late Pleistocene age for these deposits[8–10]. Based on the stratigraphic relationship of other Quaternary deposits with miliolites, a general stratigraphic framework has been worked out (Table 1). Significant amount of incision of exposed Quaternary sequences by young-order streams within the vicinity of the KHF indicates post-depositional upliftment of the area.

Evidence for Quaternary reactivation

Offsetting of Quaternary deposits is the most direct evidence for suggesting reactivation of a fault. The tectonic and geomorphic setting of the KHF with a thin cover of Quaternary sediments is ideal for preservation of such evidence. Detailed field studies were carried out in the Khari river basin, the largest river arising from the Katrol hill range and flowing towards the north, crossing the KHF (Figures 2 and 5 *a*). Detailed mapping of the Quaternary deposits, especially those overlapping the KHF fault zone was done so as to locate offsetting in these deposits as a consequence of reactivation of KHF. The Khari river shows significant amount of incision. Paired river terraces and hanging fluvial valleys have formed within the vicinity of the KHF in the Khari river basin (Figure 5 *b*).

We describe here the offsetting and deformation of Quaternary deposits observed in the Khari river basin. The location of site is shown in Figure 5 *a*. Field documentation of the site was followed by GPR surveys, as it

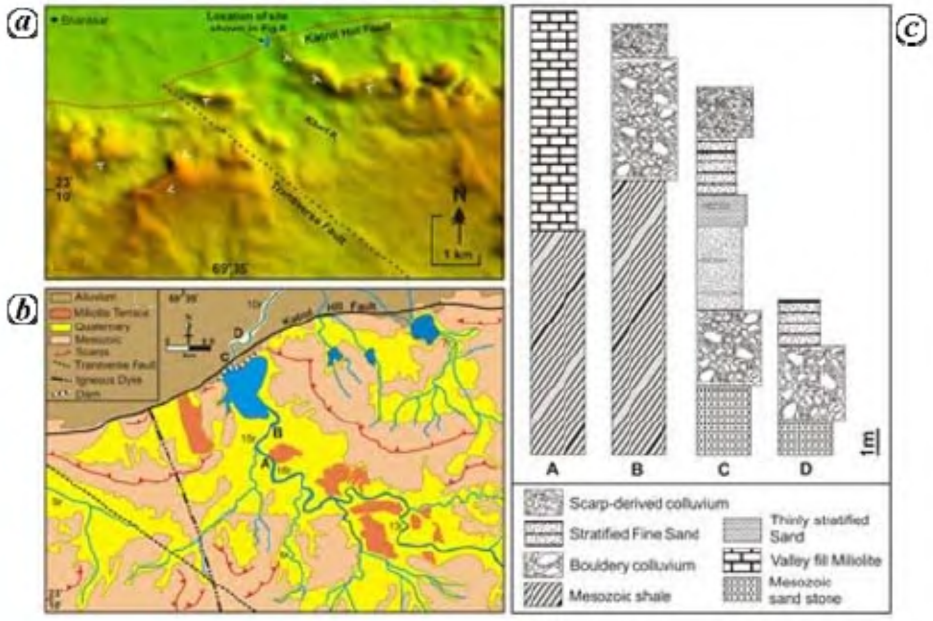

Figure 5. ***a***, SRTM data of the area south of Bharasar showing sharp geomorphic contrast across the KHF. Note variation in the dip of the scarp due to doming of the Mesozoic formations. The precise location of the KHF is marked by field and GPR investigations. Locations of the GPR survey are also shown. ***b***, Geological map of a part of the Katrol hill range showing paired miliolite terraces incised by Khari river, scarps, KHF, transverse fault and dyke. Location of the area is shown in Figure 2. ***c***, Representative lithologs of exposed Quaternary sediments along the Khari river. Lithologs A and B are located to the south of the KHF, whereas lithologs C and D are located to the north of the KHF. Location of the lithologs is shown in (***b***).

is necessary to understand the relation of the nature of KHF with younger deposits (Figure 5 *a*). This site is located along the Khari river just north of the scarpline (Figure 5 *a*). Here the Quaternary sediments are seen overlying the Mesozoic rocks. The KHF passes across the Khari river at this site and trends in NE–SW direction. The fault, exposed on the river floor, marks the lithotectonic contact between the Bhuj Formation to the north and shales of the Jhuran Formation to the south. The cliff section exhibits Mesozoic rocks overlain by 7 m thick Quaternary sediments (Figure 6). The overlying Quaternary sediments show offsetting along two faults (*F*1 and *F*2) with associated minor faults (Figures 6). Unit A comprises the oldest Quaternary deposits of bouldery colluvium, which is displaced 7 m along the SE-dipping KHF. The bouldery fragments of shale and sandstone of pre-Bhuj Formation having 40–50 cm diameter at the base of unit A show unconformable contact with the underlying south-dipping Mesozoic rocks. Total thickness of this unit is about 4 m and the size of unsorted boulders is found to gradually reduce towards the surface. The gravelly clasts of unit A are oriented along a steep-dipping fault plane prior to offset by the gentle SE-dipping KHF. The top of unit A in the SE block is at ~9 m, while the same occurs at ~2 m in the NE block (Figure 6), which gives a total vertical offset of ~7 m within the Quaternary sediments overlapping the KHF. The base of unit A is not exposed on the foot wall to the north. Thin, discontinuous, clast-rich layers are also seen in unit A. This unit correlates with the basal colluvium found to occur below the miliolites all along the KHF and is inferred to be of middle Pleistocene age (Table 1).

The overlying unit B comprises mostly sands with layers of gravelly sand. The thickness of unit B is 0.5 m in the hanging wall, which abruptly increases up to 2 m in the foot wall. Unit B shows offsetting along both the faults. Thin layers of fine gravel sandwiched within this unit also show deformation and offsetting by minor faults (Figure 6). In the foot wall, a thick layer of 0.75–1 m of coarse homogenous fluvial sands, designated as unit C, rests over unit B. This unit is missing in the hanging wall. Overlying unit C is a 1.5–1.7 m thick, well-lithified, miliolitic sand deposit named as unit D. The higher degree of compaction of this unit can be attributed to the presence of carbonate content. The continuity of unit D is also missing in the hanging wall (Figure 6). The composite sediment package comprising units B–D lithologically correlates with valley fill miliolite (Table 1) dating back to late Pleistocene (Table 1). The overlying alluvium shown in Table 1, is absent in the exposed section. The topmost layer of the section is 1.25–1.5 m thick and is named as unit E. A thin apron of unit E consisting of angular and unsorted debris correlates with the scarp-derived colluvium of late Holocene age described by Patidar *et al.*[6].

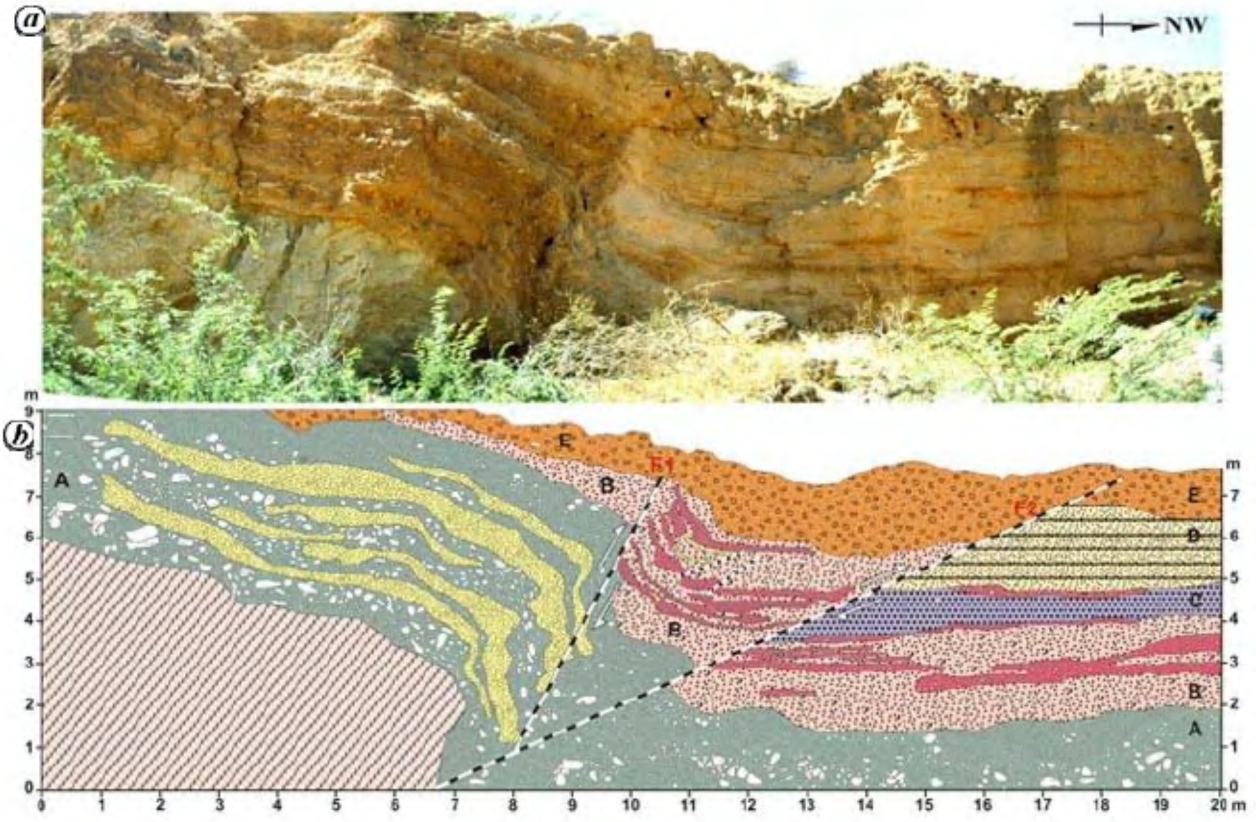

Figure 6. ***a***, Exposed cliff section along the Khari river to the SE of Bharasar showing offsetting in the Quaternary sediments along the KHF. Location of the site is shown in (***c***). ***b***, Overlay of cliff section showing various lithologies and faults. A, Bouldery colluvium; B, Gravelly sand; C, Coarse sand; D, Stratified miliolitic sand and E, Scarp-derived colluvium. Note the splaying nature of the KHF in Quaternary deposits.

This unit continues from the hanging wall to the foot wall and shows offset along *F*2 only (Figure 6).

The various units described above show erosional bases. However, the major erosional contacts are between units A and B, as well as between D and E. These mark major phases of erosion, which serve to categorize the total observed offset into discrete events of faulting. Accordingly, three events or phases of reactivation of the KHF have been delineated. The first event post-dates the deposition of unit A (Event 1), which led to the formation of the steeper fault (*F*1) as a consequence of upward propagation of the KHF, followed by the development of erosional surface over it. This was followed by deposition of fluvial sediments comprising units B, C and D, with minor breaks in sedimentation. The second event occurred after the deposition of unit D (Event 2), which was again followed by erosion. During this event, the second fault with gentler dip (*F*2) was formed. However, the offset related to this event was recorded along both faults. The wedge formed between the two faults resulted in the preservation of a major part of unit B, which also shows several sympathetic minor faults. The overlying units C and D and major part of unit B were not observed in the hanging wall due to post-faulting erosional activity. Over this erosional surface, unit E which comprises scarp-derived colluvium was deposited. The offset observed in this unit along both faults forms the third event of faulting (Event 3). During each of the three faulting events, the KHF clearly appears to have displaced the then existing topographic surfaces as it propagated upwards. Based on the correlation of the offset sediments with the available stratigraphic set-up of Quaternary deposits (Table 1), we suggest that Event 1 occurred sometime in late Pleistocene, while Events 2 and 3 are tentatively bracketed to early Holocene and < 2 ka respectively. The deformation observed in the Quaternary sediments is the cumulative effect of repeated faulting along the two south-dipping reverse faults (*F*1 and *F*2).

GPR investigations along KHF

The GPR technique was employed to map the active fault strand of the KHF in the shallow subsurface and the

change in geometry as it propagates upwards in the younger Quaternary deposits. GPR is an emerging high-resolution geophysical technique to appraise the shallow subsurface stratigraphy and neotectonics[11–13]. In the GPR, high-frequency electromagnetic waves are used to produce the continuous cross-sectional profile or records of subsurface features, without destruction. GPR is a time-dependent geophysical technique that can provide a 3D pseudo image of the subsurface and can also provide accurate depth estimates for many common sub-surface objects; it gives a more direct image of the subsurface.

The use of GPR has been established to demarcate the shallow geometry of the fault plane/zone, which is otherwise difficult to understand. Successful results for tectonic studies using GPR have been obtained by various workers[6,7,14–23]. GPR data are useful to identify the nature and geometry of the tectonic structures beneath tens of metre from the surface with a high resolution continuous image. Precise mapping of the associated subsurface deformational features can help build the tectonic history of the area[13]. Studies of deformed Quaternary sequences are vital to appreciate the recent behaviour of the fault. To further strengthen the field data, we carried out subsurface studies across the KHF using GPR. The preliminary aim was to identify subsurface geometry of the KHF and its upward propagation in Quaternary sediments and associated deformational pattern. We adopted different methods of data collection with a combination of data-acquisition parameters to acquire precise subsurface image of the area.

A 25 m long GPR profile was raised in the NW–SE direction by dragging the 200 MHz frequency antenna (GSSI-make) on the top of the cliff section shown in Figure 6, as is the usual practice followed in GPR surveys, several profiles were obtained out of which the best one was processed and interpreted. The GPR profile shows offsetting of the reflections along a gentle dipping plane marked as KHF (Figure 7). The upward propagation of the fault plane is clearly seen in the GPR profile. Extensive hyperbolic reflections represent deformation along the fault plane and the presence of angular to sub-angular bouldery colluvium deposits at the middle part of the profile. The GPR data show interesting information about the subsurface geometry of the fault plane and associated features (Figure 7). The splaying nature of the main fault strand towards the surface is obvious in the GPR profile. The dip of the KHF progressively decreases as it propagates upward from the Mesozoic to Quaternary sediments. Since the KHF indicates similar stress conditions from Mesozoic rocks below to Quaternary sediments above, this may be attributed to changes in rheology of the overlying rocks and the ongoing stress regime. The radar reflections from the upper part of the profile are correlated with the exposed section shown in Figure 6.

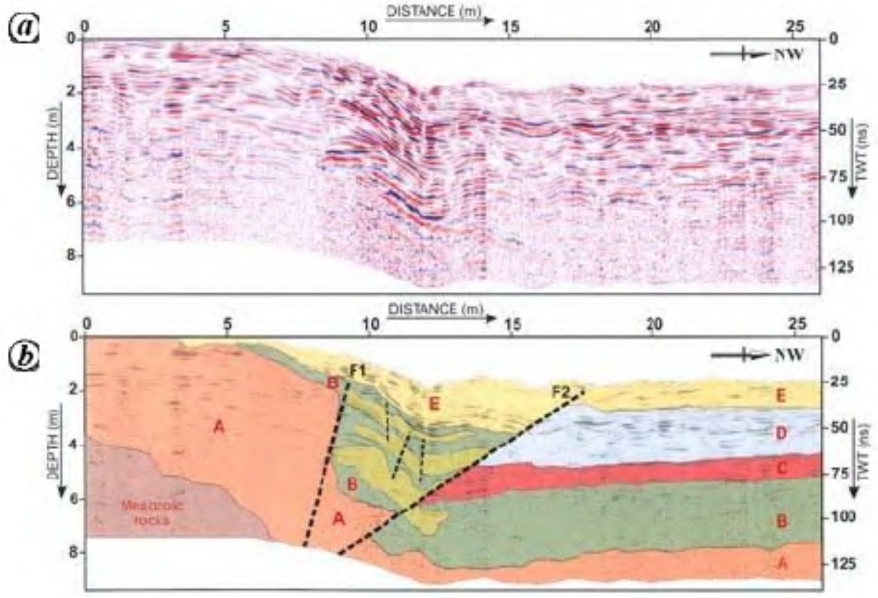

Figure 7. GPR profile showing active fault strand of the KHF. Location of the survey site is given in Figure 5. ***a***, High-resolution, topographically corrected GPR profile in line-scan mode raised by 200 MHz centre frequency monostatic antenna showing scattering of signals due to SE-dipping fault. ***b***, Overlay of GPR profile shown in (***a***). The units are characterized on the basis of specific reflection patterns and their correlation with exposed cliff section. A, Bouldery colluvium; B, Gravelly sand; C, Coarse sand; D, Stratified miliolitic sand and E, Scarp-derived colluvium. Splaying nature of the KHF is also clear in GPR data. Note the offsetting and deformation by minor faults.

The faulting observed in the sediments is marked by offset reflectors. The fault is marked as a reverse fault dipping 40° due SE. Scattering in the radar signals seen along the fault plane is due to a change in lithology across the plane. The interpreted reflection patterns of the Quaternary sediments and the underlying Mesozoic rocks are used to interpret the other GPR profiles raised over the flat ground.

Discussion

The KHF is a E–W-trending intrabasinal fault in the Mainland Kachchh that marks the lithotectonic contact between the Bhuj Formation to the north and older Mesozoic formations to the south[24]. The north-facing scarps, incised river courses, fluvial hanging valleys and development of narrow gorges along the Khari river on either side of the KHF indicate differential uplift of the area[6]. Geomorphologic data and the offsetting in Quaternary sediments provide unequivocal evidence for reactivation of the KHF in the recent past. Offset in Quaternary sediments recorded at two sites located exactly above the KHF fault line conclusively proves its upward propagation. Site 1 demonstrates that the observed deformation and offset is the cumulative effect of multiple events along the KHF. The total vertical offset within the Quaternary sediments is about 7 m. Based on the stratigraphy of the various horizons, at least three events are discernible as described earlier. The events can be tentatively bracketed in geologic time based on the correlation of the affected sediments with the available stratigraphic set-up (Table 1). Event 1 occurred sometime in the late Pleistocene, while Event 2 occurred during early Holocene. Event 3 is younger than 2 ka. It is significant to note that the KHF propagated up to the surface during each of the three faulting events. Each faulting event was followed by erosion of sediments from the southern block.

Studies carried out so far have suggested that the KHF is a south-dipping reverse fault and is offset by various transverse trending faults[5–7]. Field studies carried out in this study show that the dip of the fault varies considerably from east to west (Figure 3). At Khatrod in the eastern part, the KHF is observed to show steep dips up to 80° towards the south, while in the western part near Samatra, the KHF shows a 45° dip due south within the Mesozoic rocks (Figure 3). However, the upward extension of the KHF in Quaternary sediments observed at sites 1 and 2 shows gentler dips (Figures 6 and 7). The KHF has been identified as a growth fault during the Quaternary deposition and the splaying of the main fault strand is also noticed. The results of GPR also point to changes in the nature of the fault during its upward propagation in Quaternary sediments. The reverse movements along the KHF and its splaying nature in Quaternary sediments indicate its neotectonic reactivation in compressive stress regime.

Conclusions

The geomorphic set-up of the KHF provides ample evidence of neotectonic activity. Periodic reactivation of the KHF is recorded as offsetting within Quaternary sediments overlapping the fault line. At least three events of faulting are indicated which are related to three faulting events during the late Quaternary. Each of these events had offset the then existing topographic surface as well. Based on the stratigraphy of Quaternary sediments, we suggest that Event 1 occurred sometime in the late Pleisotocene, while Events 2 and 3 occurred in the early Holocene and <2 ka respectively. Field observations and GPR investigations point towards splaying of the KHF within the Quaternary sediments as it propagated upwards under compressive stress conditions.

1. Biswas, S. K., Mesozoic rock stratigraphy of Kutch. *Q. J. Geol. Min. Metall. Soc. India*, 1977, **49**, 1–52.
2. Biswas, S. K., Regional tectonic framework, structure and evolution of western marginal basins of India. *Tectonophysics*, 1987, **135**, 307–327.
3. Biswas, S. K., Landscape of Kutch – A morphotectonic analysis. *Indian J. Earth Sci.*, 1974, **1**, 177–190.
4. Biswas, S. K. and Khattri, K. N., A geological study of earthquakes in Kachchh, Gujarat, India. *J. Geol. Soc. India*, 2002, **60**, 131–142.
5. Maurya, D. M., Thakkar, M. G. and Chamyal, L. S., Implications of transverse fault system on tectonic evolution of Mainland Kachchh, western India. *Curr. Sci.*, 2003, **85**, 661–667.
6. Patidar, A. K., Maurya, D. M., Thakkar, M. G. and Chamyal, L. S., Fluvial geomorphology and neotectonic activity based on field and GPR data, Katrol hill range, Kachchh, western India. *Quat. Int.*, 2007, **159**, 74–92.
7. Maurya, D. M. *et al.*, Need for initiating ground penetrating radar studies along active faults in India: An example from Kachchh. *Curr. Sci.*, 2005, **88**, 231–240.
8. Baskaran, M., Deshpande, S. V., Rajaguru, S. N. and Somayajulu, B. L. K., Geochronology of miliolite rocks of Kutch, western India. *J. Geol. Soc. India*, 1989, **33**, 588–593.
9. Chakrabarti, A., Somayajulu, B. L. K., Baskaran, M. and Kumar, B., Quaternary miliolites of Kutch and Saurashtra, western India: Depositional environments in the light of physical sedimentary structures, biogenic structures and geochronological setting of the rocks. *Senckenbergaina Marit.*, 1993, **23**, 7–28.
10. Somayajulu, B. L. K., Age and mineralogy of the miliolites of Saurashtra and Kachchh, Gujarat. *Curr. Sci.*, 1993, **64**, 926–928.
11. Anderson, K. B., Spotila, J. A. and Hole, J. A., Application of geomorphic analysis and ground-penetrating radar to characterization of paleoseismic sites in dynamic alluvial environments: An example from southern California. *Tectonophysics*, 2003, **368**, 25–32.
12. Gross, R., Green, A., Holliger, K., Horstmeyer, H. and Baldwin, J., Shallow geometry and displacement on the San Andreas Fault near Point Arena based on trenching and 3-D georadar surveying. *Geophys. Res. Lett.*, 2002, **29**, 34(1–4).
13. Rashed, M., Kawamura, D., Nemoto, H., Miyata, T. and Nakagawa, K., Ground penetrating radar investigations across the Uemachi fault, Osaka, Japan. *J. Appl. Geophys.*, 2003, **53**, 63–75.
14. Busby, J. P. and Meritt, J. W., Quaternary deformation mapping with ground penetrating radar. *J. Appl. Geophys.*, 1999, **41**, 75–91.
15. Cai, J., McMechan, G. A. and Fisher, M. A., Application of ground penetrating radar to investigation of near surface fault

properties in the San Francisco Bay region. *Bull. Seismol. Soc. Am.*, 1996, **86**, 1459–1470.
16. Gross, R., Green, A. and Horstmeyer, H., Location and geometry of the Wellington Fault (New Zealand) defined by detailed three-dimensional georadar data. *J. Geophys. Res.*, 2004, **109**, B05401 (1-14).
17. Liner, C. L. and Liner, J. L., Application of GPR to a site investigation involving shallow faults. *Leading Edge*, 1997, **16**, 1649–1651.
18. Maurya, D. M., Goyal, B., Patidar, A. K., Mulchandani, N., Thakkar, M. G. and Chamyal, L. S., Ground Penetrating Radar imaging of two large sand blow craters related to the 2001 Bhuj earthquake, Kachchh, western India. *J. Appl. Geophys.*, 2006, **60**, 142–152.
19. Meschede, M., Aspiron, U. and Reicherter, K., Visualisation of tectonic structures in shallow-depth high-resolution ground penetrating radar (GPR) profiles. *Terra Nova*, 1997, **9**, 167–170.
20. Mulchandani, N., Patidar, A. K., Vaid, S. I. and Maurya, D. M., Late Cenozoic geomorphic evolution in response to inversion: Evidence from field and GPR studies in Kim drainage basin, western India. *J. Asian Earth Sci.*, 2007, **30**, 33–52.
21. Patidar, A. K., Maurya, D. M. and Chamyal, L. S., Shallow subsurface characterization of active faults using Ground Penetrating Radar: Example from Katrol Hill Fault (KHF), Kachchh, western India. In Proceedings of the Eleventh International Conference on Ground Penetrating Radar (GPR 2006), The Ohio State University, USA, 19–22 June 2006.
22. Salvi, S., Cinti, F. R., Colini, L., Addezio, G. D., Doumaz, F. and Pettinelli, E., Investigation of the active Celano-L'Aquila fault system, Abruzzi (Central Appennines, Italy) with combined ground penetrating radar and palaeoseismic trenching. *Geophys. J. Int.*, 2003, **155**, 805–818.
23. Young, R. A., Stewart, S. C., Seman, M. R. and Evans, B. J., Fault-plane reflection processing and 3D display: The Darling Fault, Western Australia. *Tectonophysics*, 1990, **173**, 107–117.
24. Biswas, S. K. and Deshpande, S. V., Geologic and tectonic maps of Kachchh. *Bull. Oil Nat. Gas Comm.*, 1970, **7**, 115–116.

ACKNOWLEDGEMENT. We thank the Department of Science and Technology, New Delhi, for funding a GPR-based research project.

Received 27 March 2007; revised accepted 5 October 2007